REPORT DOCUMENTATION PAGE

Form Approved OMB No. 0704-0188

maintaining the data needed, and completing and reviewing the collection of information. Send comments regarding this burden estimate or any other aspect of this collection of information, including suggestions for reducing the burden, to Department of Defense, Washington Headquarters Services, Directorate for Information Operations and Reports (0704-0188), 1215 Jefferson Davis Highway, Suite 1204, Arlington, VA 22202-4302. Respondents should be aware that notwithstanding any other provision of law, no person shall be subject to any penalty for failing to comply with a collection of information if it does not display a currently valid OMB control number.
PLEASE DO NOT RETURN YOUR FORM TO THE ABOVE ADDRESS.

1. REPORT DATE *(DD-MM-YYYY)*	2. REPORT TYPE	3. DATES COVERED *(From – To)*
28-01-2002	Final Report	29 August 2000 - 26-Mar-02

4. TITLE AND SUBTITLE

First principle calculations of electrical levels for radiation induced defects in SiO2

5a. CONTRACT NUMBER
F61775-00-WE059

5b. GRANT NUMBER

5c. PROGRAM ELEMENT NUMBER

6. AUTHOR(S)

Dr. Alexander L Shlyuger

5d. PROJECT NUMBER

5d. TASK NUMBER

5e. WORK UNIT NUMBER

7. PERFORMING ORGANIZATION NAME(S) AND ADDRESS(ES)

University College London
Gower Street
London WC1E 6BT
United Kingdom

8. PERFORMING ORGANIZATION REPORT NUMBER

N/A

9. SPONSORING/MONITORING AGENCY NAME(S) AND ADDRESS(ES)

European Office of Aerospace Research and Development
PSC 802 BOX 14
FPO 09499-0014

10. SPONSOR/MONITOR'S ACRONYM(S)

EOARD

11. SPONSOR/MONITOR'S REPORT NUMBER(S)
SPC 00-4059

12. DISTRIBUTION/AVAILABILITY STATEMENT

Approved for public release; distribution is unlimited.

13. SUPPLEMENTARY NOTES

14. ABSTRACT

This report results from a contract tasking University College London as follows: The contractor will investigate electrical levels for radiation induced defects in amorphous SiO2. The objectives of this project are: 1) To develop an embedded cluster method for calculations of the electronic structure and spectroscopic properties as well as electron affinities and ionization potentials of point defects in crystalline and amorphous silica; 2) To study the geometric electronic structure, stability and properties of proton and H- centers in a-quartz and amorphous silica.

20020927 170

15. SUBJECT TERMS
EOARD, Electronic Devices, Space Technology

16. SECURITY CLASSIFICATION OF:			17. LIMITATION OF ABSTRACT	18, NUMBER OF PAGES	19a. NAME OF RESPONSIBLE PERSON
a. REPORT	b. ABSTRACT	c. THIS PAGE			Carl A. Kutsche
UNCLAS	UNCLAS	UNCLAS	UL	14	19b. TELEPHONE NUMBER *(Include area code)* +44 (0)20 7514 4505

EOARD CONTRACT No F61775-00-WE059

First principle calculations of hydrogen defects in a-SiO_2

FINAL REPORT

A. L. Shlyuger and P. V. Sushko

1. Introduction

Amorphous silicon dioxide (a-SiO_2) comprises the gate and passivation oxide layers in most MOS devices. However, the current understanding of defects induced in a-SiO_2 due to high-energy radiation in space is inadequate for making predictions about various options for device fabrication. It is also inadequate for interpretation of results of radiation testing of critical components of Air Force Space Systems. Theoretical modelling plays an important role in developing models and elucidating properties of these defects. However, computational methods currently available for *ab initio* calculations of defects in amorphous solids are not fully adequate for predictive modelling. They fall into two major groups. In the first group, an infinite amorphous structure is represented by periodic translation of an amorphous unit cell. These methods often employ *ab initio* Molecular Dynamics to generate an amorphous structure and then use the same computational technique in static mode to study defects in this structure (see, for example, refs. [1-3]). In the second group, amorphous structure is represented by a finite cluster saturated at the border by Hydrogen atoms or model pseudo-atoms [4]. Small molecular clusters used in most *ab initio* calculations cannot account for both the Madelung potential in amorphous structure and the long-range structural relaxation induced by a defect. These clusters are either cut out from a larger fragment of an amorphous structure (see section 2) or artificially constructed from general considerations to model the defect environment. The periodic approach is more consistent in a sense that the same *ab initio* method can be used to produce the amorphous structure and to study defect properties. However, a*b initio* calculations of periodic systems are time-consuming and therefore consider small periodic cells. This does not allow one to fully account for the intermediate and long-range order in amorphous structures [5,6].

An alternative approach is an embedded cluster model where single defect is treated in *infinite* polarizable lattice. A hybrid method developed in our group at UCL [7-11] combines quantum mechanical treatment of atoms surrounding a defect with the classical representation of the rest of the solid in a shell model [12]. It has been widely used to study point defects in ionic crystals. This approach naturally account for both the Madelung potential at the site of interest and the ionic and electronic polarisation of the system by the defect. In the EOARD funded contract No F61775-00-WE001 we extended the embedded cluster method to include ionic-covalent systems, such as crystalline SiO_2. The main aim of this project was to develop this method further that it could treat disordered (amorphous) SiO_2. This involved: 1) developing of a computer code for comprehensive analysis of amorphous structures; and 2) extending the embedded cluster approach to calculation of localised defects in amorphous SiO_2, and making test applications to charged Hydrogen defects: proton (H^+) and H^- centers.

2. Details of calculations

Unlike in crystalline structures, all sites in amorphous structures are different and one should generally study distributions of defect properties over many different sites. On the other hand, some sites may

DISTRIBUTION STATEMENT A
Approved for Public Release
Distribution Unlimited

AQ F02-12-3357

have specific properties, which make them particularly important for applications. For example, three and four-member rings in amorphous SiO_2 are thought to be responsible for the low-energy optical absorption tail which can be selectively excited by 7.9 eV photons of F_2 laser [13]. Therefore the general strategy of embedded cluster calculations of defects in a-SiO_2 includes: i) generating amorphous structures; ii) characterizing obtained structures in terms of distributions of various structural parameters, and finding particular sites interesting for defect studies; iii) constructing quantum clusters at different sites and calculating defect properties; iv) building a statistics of defect properties over many sites and producing distributions of defect properties (see, for example, ref. [14]). The main objective of this project was to build computational methods for each stage of this program and to test them on a particular system. These methods are discussed in detail below.

Preparation of amorphous structures. Several methods have been used in the literature for generating a-SiO_2 structures (see, for example, refs. [5,6,15]). In this work we resorted to the most commonly employed classical molecular dynamics technique [16,17]. This technique can be used to model melting and cooling process of some crystalline SiO_2 polymorph and in this way to mimic a process of glass formation in laboratory conditions. It is particularly convenient for our applications as it is compatible with the embedded cluster method where the same classical atomistic simulation technique is used for representing the rest of the amorphous structure surrounding a defect treated quantum-mechanically.

The molecular dynamics (MD) simulations of the glass formation were made in the periodic model using the DL_POLY computer code [18]. The crystalline β-crystobalite is a convenient choice of initial structure due to its cubic lattice cell. The classical inter-atomic potentials used in this study were developed in ref. [19] using the results of *ab initio* calculations of small SiO_2 clusters. These potentials reproduce accurately the relative stability of several SiO_2 polymorphs and have been used in several previous studies of SiO_2 glasses [17]. The glass preparation procedure is summarized below.

i) Two super-cells of β-crystobalite of 192 and 648 atoms were heated relatively fast (at approximately $4 \cdot 10^{13}$ K/s) at constant normal pressure to high temperature (T_{high} = 7000K).
ii) The system was kept at T_{high} for approximately 100 ps, which is significantly longer than is required to achieve thermal equilibrium.
iii) The equilibrated system was cooled down to 0K or 300K with a relatively small cooling rate, which is sufficient to provide convergence of characteristic glass properties [17]. The slowest cooling rate used in this study was 10^{12} K/s.
iv) Finally, the thus produced structures were relaxed using a static energy minimization technique.

Several amorphous structures were obtained using this procedure and different cooling rates and other parameters of molecular dynamics. The main characteristics of these structures were analyzed using the method described below and are discussed in section 3.

Analysis of amorphous structures is required to: i) compare different amorphous structures; ii) identify potential traps for electrons, holes and excitons in the 'non-defective' amorphous structure; and iii) correlate local properties of amorphous structure with defect properties, such as optical excitation and defect formation energies. Out of several amorphous structures generated by the method described above we have chosen only those structures which had ideal connectivity and thus corresponded to the continuous random network model of ideal glass [5,6]. The latter assumes the ideal 4-2 coordination, i.e. each Si atom is coordinated by four Oxygen atoms and each O atom is coordinated by two Silicon atoms. The experimental interference and correlation functions deduced

from neutron diffraction data provide information about three different ranges of order in the amorphous structure [6]. Range I (short-range of *ca.* 1-2 Å) describes the local geometrical parameters such as Si–O inter-atomic distances and O–Si–O tetrahedral angles. Range II (medium range of *ca.* 2-5 Å) includes parameters such as Si–Si inter-atomic distances and torsion angles, which describe relative orientation of neighboring SiO_4 tetrahedral units. Range III corresponds to long-range order at *ca.* 5-15 Å from the center of interest. We should note that both the experimental and theoretical methods rely on a number of approximations. In particular, inter-atomic potentials are fitted to reproduce crystal structure and relative energies of different SiO_2 polymorphs. These potentials are best defined in a region close to the equilibrium separation between atoms in a crystal and, therefore, may not necessarily reproduce the SiO_2 melt. Also the typical size of a system and timescale of presently available MD simulations are many orders of magnitude smaller than those in real life processes, which represents a principal difficulty. Nevertheless, it is presently accepted that thus obtained amorphous structures are representative of real amorphous systems and therefore it is essential to have a tool for comprehensive analysis of their properties.

In this project, we developed a computer code PAS (Portrait of an Amorphous System) for geometric and correlation analysis of crystalline and amorphous SiO_2 structures. The code is currently applicable to systems with the ideal 4-2 coordination and can be easily extended to systems with non-ideal coordination too. It inputs parameters of the unit cell, fractional or Cartesian coordinates of unit cell atoms and values of on-site electrostatic potential. It first determines a table of nearest neighbors (TNN) using the "smallest distance" criterion (e.g. O atoms at the distance less than 1.8 Å from a Si atom are taken as its nearest neighbors). The number of characteristics is then calculated using the TNN:

i) distributions of Si–O and Si–Si inter-atomic distances;
ii) distributions of Si–O–Si and O–Si–O angles;
iii) electrostatic potential distribution;
iv) pair-wise distribution functions g(Si-O), g(O-O), g(Si-Si);
v) number of different rings in the system.

The PAS code also performs analysis of the ring structure and correlates the properties i) – iii) of ring atoms with the size of the ring. In addition the PAS code generates an input for embedded cluster calculations using the GUESS code.

Analysis of rings in a-SiO_2 is often used as a tool for characterizing the properties of amorphous structures. Structure of many ion-covalent and covalent materials, in general, and SiO_2 polymorphs, in particular, allows for closed paths (rings) within the system. The number and size of rings in different SiO_2 polymorphs is associated with their structure and density [5]. Statistics and structure of rings in a-SiO_2 is of considerable interest because small planar rings are thought to determine the mobility edge and the optical absorption tail in real glasses [13,20] and larger-size rings are responsible for gaseous permeability and diffusion of defect species. The small 3- and 4-member rings have also been associated with specific peaks (D_1 and D_2) in the Raman spectrum [2,3].

There are two most commonly used definitions of a ring. One of them defines a ring associated with an atom Si_i as a shortest path $Si_i - O_{ij} -...- O_{ik} - Si_i$, where O_{ij} and O_{ik} are nearest neighbors of Si_i and $j \neq k$. According to this definition each Si atom has 6 rings associated with it. We have adopted another definition in which a ring is defined as a closed path without shortcuts, i.e. without any path from one atom of the ring to the other being shorter than the ring path. The two definitions are not identical, but the second definition seems more meaningful because it regards a ring as an entity, a particular feature

of the glass structure, while the first one considers rings in the mathematical sense as a number of closed paths associated with each atom.

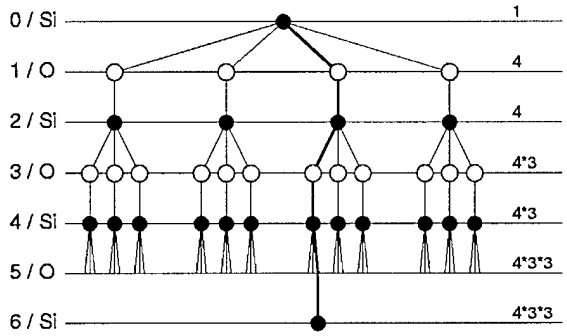

Fig. 1. Tree of neighbors for a root Si atom at the top of the figure. Black and white circles arranged in levels are Si and O atoms respectively. The level number is shown on the left; values on the right show the total number of atoms in each level. The bold line shows a closed 3-member path found for the root Si atom: the path includes Si atom at level 6 (the same atom as at level 0) and two other Si atoms at levels 4 and 2 and corresponding Oxygen atoms.

Analysis of the ring statistics in a-SiO_2 is a complex computational problem. To explain the algorithm of ring search implemented in the PAS code we will refer to Figs. 1 and 2. The search for rings begins with construction of a tree of neighbors for each Si atom, as shown in Fig. 1. In such a tree the 'root" Si atom occupies level 0 and further levels are occupied by oxygen and silicon atoms in sequential order. The tree is built so that to include sufficiently large number of shells of neighbors (up to 20 levels in our calculations). Each atom in each Si level ($Si_{level,vertix}$) is then compared with the Si atom at the root of the tree. A closed path via the root atom is found if atom $Si_{level,vertix}$ atom has the same fractional coordinates as the root atom. An example of such a path is shown in Fig. 1. The procedure is repeated for each Si atom in the unit cell. All found cycles are accumulated for further analysis.

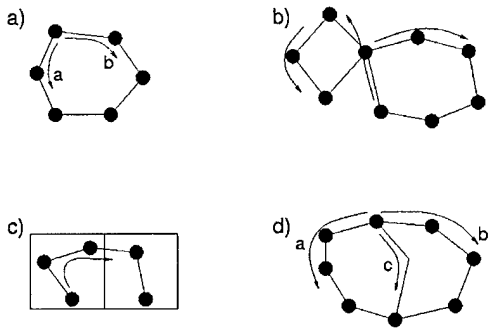

Fig. 2. Closed paths removed from the list of candidates for rings. (Only Si atoms are shown.) a) Paths **a** and **b** differ by the direction of cycling only, one of them is removed. b) At least one atom appears twice in the same path. c) The path connects the same atom in different (not necessarily adjacent) super-cells. d) Paths **c** is shorter than paths **a** or **b** (or both).

At the next step the structure and topology of all found cycles are analyzed. By construction, the list of all cycles found at the previous step is excessive, i.e. it contains many equivalent cycles and those, which do not fall under the definition of a ring. To exclude equivalent paths we note that both clockwise and anti-clockwise paths will be found for each cycle (paths **a** and **b** in Fig. 2(a)). In addition, each cycle of length n (n-member cycle, where n is the number of Si atoms) will be found n

times. This is because each *n*-member cycle will be found in *n* different trees associated with each Si atom in the cycle. Among remaining cycles the following ones have to be excluded: i) those which have any atom appearing more than once (as in Fig. 2(b)); ii) those which connect the same Si atom in different unit cells (as in Fig. 2(c)); and iii) those which have shortcuts (path **c** in Fig. 2(d) is shorter than paths **a** and **b**). The remaining cycles are called rings.

The embedded cluster method developed in our group and implemented in the GUESS computer code allows us to study point defects in crystalline and amorphous materials combining quantum mechanical treatment of a defect and its nearest surrounding with the classical shell model treatment of the rest of the solid. The GUESS method and details of its applications to point defects in crystalline SiO_2 were described in the final report to the contract NoF61775-00-WE001 and in refs. [9-11]. Here we highlight only the features specific to the present studies.

In the GUESS method, the infinite system with a single point defect is divided into several regions. A spherical region I includes: i) a quantum cluster with a defect and surrounding atoms treated quantum mechanically; ii) an interface region, which connects the quantum cluster with the rest of the solid treated classically; iii) a classical region, which includes up to several hundred atoms. Region I is surrounded by a finite region II, which is treated atomistically, and region III, which is treated in the approximation of polarisable continuum. Region III conforms geometrically to the boundary between regions I and II but extends to infinity. The classical ions in regions I and II are treated in the shell model and interact between themselves via inter-atomic potentials [19]. Note that the same inter-atomic potentials are used to generate amorphous structures using classical MD simulations. Both quantum and classical atoms in region I are allowed to relax in the course of calculations. Atoms in region II are kept fixed in their ideal, bulk positions and provide correct variations of the electrostatic potential inside the region I. Region III is used to calculate the polarization energy of the infinite lattice due to the presence of a defect in region I using the Mott-Littleton approach. One of the main advantages of this approach is that it allows us to calculate forces on quantum mechanical and classical ions and simultaneously optimize their positions using an effective energy minimization scheme.

Embedded cluster calculations of amorphous silica differ significantly from these for crystalline material. First, we note that all atoms in amorphous structures, in principle, have different local structure of their environment. Therefore, it is often impossible to use the same QM cluster to describe properties of the same defect at different sites. Then, comparison of results for the same or different defects can only be feasible if the dependence of the defect properties on the cluster size and shape is less significant than their dependence on the atomic site. In order to estimate an error introduced by the finite size of the QM cluster, and to establish grounds for comparison of the results obtained for different sites in an amorphous structure, we have studied the dependence of the results on the cluster size. To achieve that we performed calculations of the H^+ impurity center in α-quartz using two different clusters: the smaller cluster $Si_2O_7Si^*_6$ and the larger cluster $Si_5O_{16}Si^*_{12}$ shown in Figs. 3(a) and 3(b), respectively. The $Si_2O_7Si^*_6$ cluster is too small to calculate the H^- center and therefore only the $Si_5O_{16}Si^*_{12}$ cluster was used for that.

Region I+II in embedded cluster calculations may have different shapes but should be neutral with zero dipole moment. For calculations of H centers in a-SiO_2 we have chosen a spherical region I+II of the radius 30.0 Å. This region was constructed from the 648 atom supercell obtained in MD simulations and was split into $Si(O_{1/2})_4$ tetrahedral units. The latter, due to their rigid character, provide a convenient choice of structural elements in both crystalline and amorphous SiO_2. Two different regions I+II were built for a-SiO_2: one was centered on a 3-member ring and the other – on a 6-

member ring. Owing to the disordered structure the two regions have different number of atoms in them: 7912 for the 3- and 7876 for the 6-member ring. For the H centers in alpha-quartz we took region I+II built from asymmetric 9-atom unit cell repeated 14 times along each of its translation vectors. This region contains almost 25000 atoms. In all cases a spherical region I of the radius of 13.0 Å was used; however, the number of atoms in it was different for different systems: 659 and 658 for the 3- and 6-member rings respectively and 718 for alpha-quartz.

To describe accurately the structure and properties of a defect associated with a ring, it is convenient to build the corresponding QM cluster so that it includes all ring atoms and their nearest neighbors. For an n-member ring such cluster includes n Silicon atoms and n Oxygen atoms which belong to the ring, $2n$ O atoms which formally do not belong to the ring but coordinate the rings' Si atoms, and $2n$ pseudo-Si atoms which link the QM cluster with its classical environment. Such a $Si_nO_{n+2n}Si^*_{2n}$ cluster is the minimal QM cluster required to describe the ring in full. A $Si_3O_9Si^*_6$ cluster for a 3-member ring considered in this study is shown in Fig. 3(c). A similar but larger QM cluster $Si_6O_{18}Si^*_{12}$ was used to treat a 6-member ring.

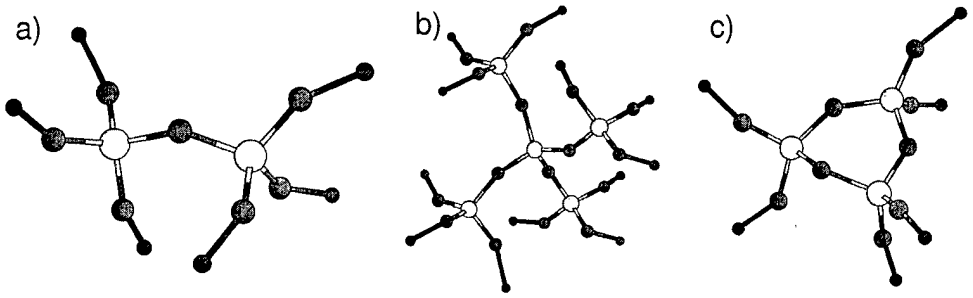

Fig. 3. (a, b) Quantum mechanical clusters $Si_2O_7Si^*_6$ and $Si_5O_{16}Si^*_{12}$ used in the calculations of H centers in α-quartz and a-SiO_2; c) $Si_3O_9Si^*_6$ – quantum cluster used to calculate the 3-member ring.

Not only QM clusters but also location of H centers within a cluster can be different. Indeed, in the case of α-quartz all sites are the same both in terms of their topology and environment. Therefore it is sufficient to consider H^+ and H^- ions bonded to one Oxygen or Silicon lattice site, respectively. In the case of a ring cluster, however, all Si or O sites of the ring are topologically equivalent but their environment is different. The latter should determine the difference is properties of the H centers. In the present study we did not investigate such dependence in details but considered only one site for each H center in one 3-member and one 6-member ring.

A standard all-electron 6-31G basis set was used to describe lattice Si and O ions in these calculations. The cc-pVDZ basis set from the Gaussian98 library was used for H ions. The interface Si* atoms, described in details in the final report to the contract NoF61775-00-WE001, were treated using a local effective core pseudo-potential and a contracted *sp* basis set.

The incorporation energies for the Hydrogen defects are calculated using:

$$E_{inc}(H^q) = (E(H^q) + E(\text{lattice})) - E(\text{lattice} + H^q),$$

where H^q is an H^+ or H^- ion. The electrostatic potential inside the region I+II is shifted with respect to that obtained by Ewald summation by V_{shift}. Values of V_{shift} are determined by the size and shape of the region I+II and can be easily calculated. The slight difference in region I+II centered at different rings results in different V_{shift}: +4.398 eV for the 3-member ring and +4.424 eV for the 6-member ring.

The value of V_{shift} for α-quartz (–3.369 eV) differs dramatically from these for amorphous silica due to a very different shape of region I+II and larger density of quartz. To compare values of E_{inc}, $IP(H^-)$ and $EA(H^+)$ calculated for different systems, these energies have to be corrected by $V_{shift} \times \Delta Q$, where ΔQ is the change of the total charge of the QM cluster in a corresponding process.

The calculated values presented in Tables 1 and 2 are corrected for V_{shift}. The Mott-Littleton correction due to the polarization of the infinite solid outside region I is about 0.3 eV and is not included into Tables 1 and 2. The frequencies of O-H and Si-H stretching modes were calculated in the harmonic approximation by diagonalizing the dynamic matrix. The latter was calculated for the displacements of the Hydrogen ion only with the electronic structure of the QM cluster being relaxed for each position of the H ion.

3. Results of test calculations

As was noted above, one of the aims of this project has been the development of computational tools for analyzing amorphous structures. The construction of the most statistically meaningful amorphous structures is a formidable task on itself, which has not been fully resolved so far [6]. The structures discussed in this chapter are obtained using the best recipes suggested in the literature on MD generating of amorphous silica structures [16,17]. They are used as representative systems to demonstrate the applicability of the developed methods to study defects in amorphous silica.

Several **glass structures** generated using the Molecular Dynamics technique were analyzed in terms of distributions of inter-atomic distances, angles between neighboring atoms, and on-site electrostatic potential. The obtained distributions are qualitatively very similar, which demonstrates that their statistical properties do not depend significantly on the parameters of MD calculations and the number of atoms in the simulation box. This is illustrated in Figs. 4 and 5 presenting the results for two structures containing 192 and 648 atoms in the simulation box, respectively. The shape and width of both distributions are very similar and are in general agreement with the results of previous theoretical modeling [16,17] and with the experimental data [6].

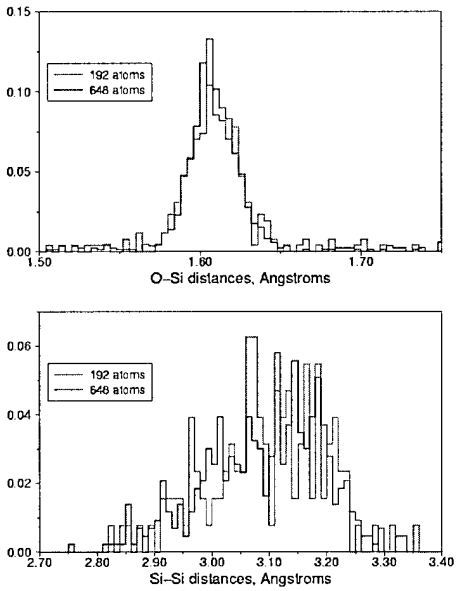

Fig. 4. Distribution of interatomic distances in structures: 192 atoms – red and 648 atoms – blue.

Using the PAS code we have also analyzed the ring statistics in five MD generated structures. Unlike α-quartz, which contains only 6- and 8-member rings, amorphous silica can be characterized by the ring distribution, which includes 3- to 8-member rings. Although the concentration of 3-member rings is relatively small, they are different from larger rings and therefore may have some special properties. For example, as was already mentioned above, they are thought to determine the tail of the optical absorption in amorphous silica [13]. On the other hand, the most abundant are 6-member rings, which are also present in all crystalline modifications of silica.

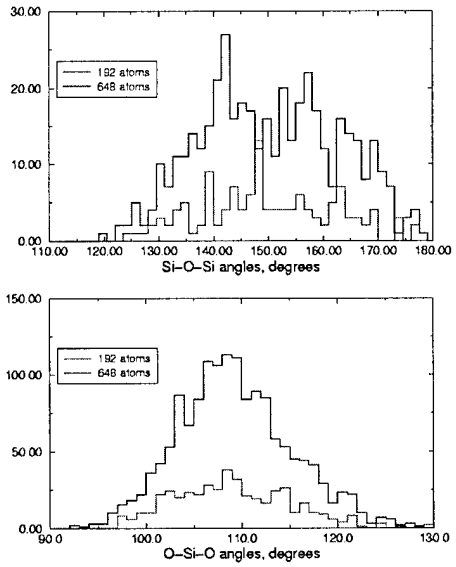

Fig 5. Distribution of Si–O–Si and O–Si–O angles for structures: 192 atoms – red and 648 atoms – blue.

Future defect studies will require more detailed analysis of amorphous structures for specific properties. For example, excitons and holes may localize only at specific sites. To find these specific sites one may need to look into the local properties such as correlations of the ring size with interatomic distances and angles associated with atoms in the ring. An example of such a correlation is presented in Figs. 6 and 7. Fig. 6 shows the distribution of distances between the atoms participating in 3- and 6-member rings. These distributions were calculated in the following way. First, information on the number and structure of rings was accumulated as discussed in the previous section. Then all atoms associated with 3-member rings were found and the distribution of inter-atomic distances was calculated. The latter step of the calculation was repeated for 6-member rings. Fig. 7 shows the distributions of angles calculated in a similar way.

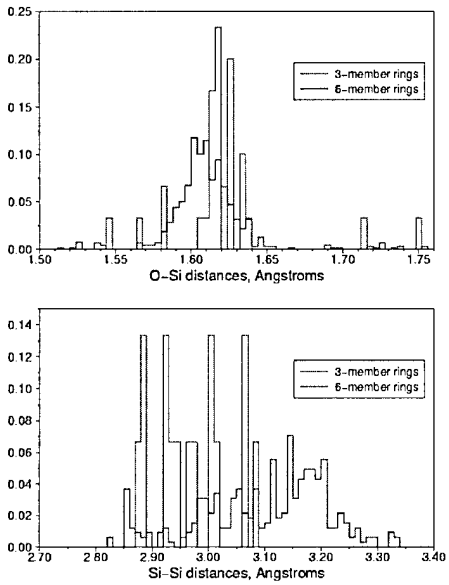

Fig. 6. Distribution of Si–O and Si–Si inter-atomic distances for 3-member rings (red) and 6-member rings (blue) within a 648-atom structure.

Closer examination of these distributions for e.g. 3-member rings allows us to deduce the following features:

i) Si–Si distances within 3-member rings are at the lower end of the distribution, i.e. they are on average about 0.10 - 0.15 Å shorter than the Si–Si distances within larger rings. It can also be seen that the maximum of the Si–Si distributions shifts to larger distances for larger, 6-member rings. However, we do not have enough statistics for more quantitative analysis.

ii) Si–O–Si and O–Si–O angles associated with 3-member rings are distinctly smaller than the angles associated with larger rings. It is possible than the same statement also applies, but to a smaller extent, to 4-member rings.

iii) There is no obvious correlation between the ring size and the on-site electrostatic potential.

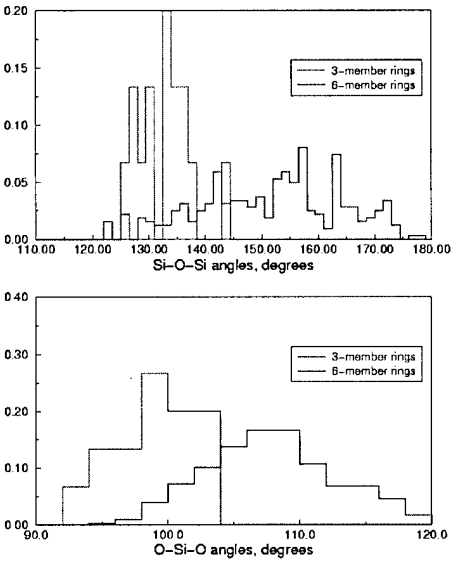

Fig. 7. Distribution of Si–O–Si and O–Si–O angles for 3-member rings (red) and 6-member rings (blue) within a 648-atom structure.

To test our embedded cluster method for **defect calculations in amorphous silica** we considered Hydrogen defects in 3- and 6-member rings in the largest 648-atom amorphous structure. The calculated properties of H^+ and H^- centers associated with a 3-member ring and a 6-member ring are summarized in Tables 1 and 2 respectively. The properties of these centers in α-quartz calculated using the same method are also included for comparison. To consider the effect of different types of local environment on the properties of H centers, we report a range of their characteristics including formation energies, parameters of the local atomic structure, vertical electron affinities and ionization potentials, harmonic frequencies of H ion vibrations. To analyze the local electronic structure of the H centers we also report atomic charges, which demonstrate strong electron density redistribution. The atomic charges are given for Hydrogen atom, the nearest neighbor O or Si atoms (in the case of H^+ or H^- centers, respectively), and for one of the second nearest neighbor atoms. The values of vertical defect ionization energies and electron affinities were calculated in two ways: with frozen shells (unrelaxed) on the atoms surrounding the QM cluster and including the shell relaxation (relaxed). The latter simulates the effect of the electronic polarization of these atoms and is included for comparison.

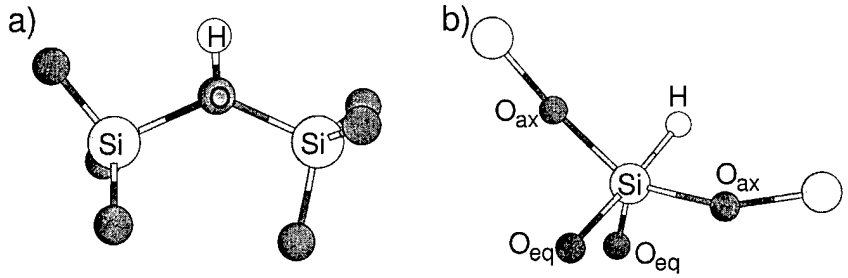

Fig. 8. Local atomic strictures of the H^- and H^+ centres in both α-quartz and a-SiO_2. See Tables 1 and 2 for comparison of the geometrical parameters.

We have calculated properties of the H^+ center in α-quartz using QM clusters $Si_2O_7Si^*_6$ and $Si_5O_{16}Si^*_{12}$. The results of these calculations (see Table 1) suggest that the dependence of the results on the cluster size is, indeed, rather small. Thus we expect that the difference in the shape and size of QM clusters used in calculating the defect properties in a-SiO_2 will not bring significant uncertainty to our results for the H^+ centers in 3- and 6- member rings. The estimated errors are about 0.2 eV for formation energies and about 0.1 eV for vertical electron affinities. We expect that similar estimates will be true for the H^- center as well, but more studies are needed to confirm this assertion.

Our results for the H^+ center suggest that the defect properties depend significantly on particular site in amorphous structure. Without further studies we could not establish any systematic pattern of the dependence of defect properties on the ring size. Nor can we state which of the two rings studied can better match the local properties of α-quartz. Indeed, the formation energies of the H^+ center in α-quartz and the 3-member ring are almost identical, while the 6-member ring gives the much lower formation energy. On the other hand, the electron affinities of the H^+ center in α-quartz and the 6-member ring are very close, while that for the 3-member ring is almost 1 eV higher. Finally, the O-H stretch vibrational frequencies are similar for the H^+ center in the 3- and 6-member rings and by about 150 cm^{-1} higher than in quartz.

Comparison of the O-H and Si-H stretching frequencies for different H^+ and H^- centers in Tables 1 and 2 shows that the variations of Si-H frequencies are much smaller than the variations of O-H frequencies. Similarly, the differences in geometrical parameters (see Fig. 8) for different H^- centers

are significantly smaller those for the H^+ centers. This can be rationalized if we note that SiO_4 tetrahedral units are very rigid. Therefore, a defect associated with such a unit, H^- for example, is "protected" from the rest of the solid. On the contrary, the H^+ center is associated with an Oxygen atom connecting two SiO_4 units, which can be relatively easily rotated with respect to each other. Therefore, the properties on H^+ center are determined by relative positions of at least two tetrahedra.

Table 1. Properties of H^+ centers in α–quartz and a-SiO_2.

Property		α-quartz		3-mem ring	6-mem ring
		$Si_2O_7Si^*_6$	$Si_5O_{16}Si^*_{12}$	$Si_3O_9Si^*_6$	$Si_6O_{18}Si^*_{12}$
$E_{incorporation}$, eV		-9.374	-9.588	-9.521	-14.467
Local geometry, Å / deg	d(O-H)	0.985	0.983	0.972	0.967
	β(Si–O–Si)	134.6	135.2	130.2	122.1
Vertical EA, eV	unrelaxed	2.474	2.367	3.037	2.249
	relaxed	3.048	2.891	3.606	2.727
ω (H^+), cm^{-1}	O-H stretching	3530.7	3602.1	3740.9	3788.6
Atomic charges (ground state), |e|	H	0.645	0.636	0.617	0.614
	O	-1.189	-1.195	-1.177	-1.192
	Si	2.845	2.834	2.803	2.835
Atomic charges (after *e-* trapping), |e|	H	0.609	0.601	0.603	0.594
	O	-1.174	-1.184	-1.166	-1.181
	Si	2.364	2.359	2.285	2.332

Table 2. Properties of H^- centers in α–quartz and a-SiO_2.

Property		α-quartz	3-mem ring	6-mem ring
		$Si_5O_{16}Si^*_{12}$	$Si_3O_9Si^*_6$	$Si_6O_{18}Si^*_{12}$
$E_{incorporation}$, eV		3.324	4.931	9.247
Local geometry, Å / deg	d(O-H)	1.455	1.449	1.442
	$\beta(O_{ax}–Si–O_{ax})$	169.8	172.8	168.7
	$\beta(O_{eq}–Si–O_{eq})$	106.2	107.6	107.0
Vertical IP, eV	unrelaxed	7.189	6.758	7.129
	relaxed	6.741	6.299	6.772
ω (H^-), cm^{-1}	Si-H stretching	2336.6	2347.8	2389.3
Atomic charges (ground state), |e|	H	-0.255	-0.253	-0.286
	Si	2.340	2.344	2.387
	O	-1.315	-1.320	-1.308
Atomic charges (ionised state), |e|	H	-0.007	-0.151	-0.070
	Si	2.256	2.277	2.332
	O	-0.772	-0.586	-0.708

We would like to point out that the H centers discussed above do not only differ by their environment Different QM clusters, both in terms of their topology and size, were used in our calculation. The latter must contribute to some extent to the spread of values presented in Tables 1 and 2. However, from our experience with the neutral Oxygen vacancy in α–quartz, the dependence of the formation energies on the cluster size is quite small [11]. Therefore, preliminary we can conclude that variations in properties of localized defects, such as H^+ and H^- centers at different sites of SiO_2 polymorphs and in a-SiO_2, are due to differences in their environment at ranges II and III. The local atomic structure and charge

density of these defects are essentially independent on the details of their environment. Finally, we note that an n-member ring can potentially accommodate n different H^+ centers and up to $6n$ different H^- centers. Therefore, further calculations are needed to understand better whether properties of localized defects such as H^+ and H^- centers correlate with the ring size and, more generally, with their short-, medium-, and/or long-range environment (ranges I, II, and III respectively).

4. Summary and conclusions

In this project we developed computational tools for analysis of amorphous structures and extended the embedded cluster approach to study localized defects in amorphous SiO_2. The PAS code allows one to fully characterize amorphous structures in terms of distributions of bond-lengths, angles, rings and other structural parameters. It also allows one to correlate local geometric parameters of amorphous structures with electrostatic potential and search for particular structural features. The embedded cluster method, in its turn, allows one to perform accurate quantum mechanical calculations of selected defect sites and their local environment and to account classically for the short- and long-range response of the rest of the amorphous network. This method is self-consistent in a sense that a QM cluster is built as a fragment of an amorphous structure and remains coupled to the amorphous network throughout the calculation. Moreover, the classical environment of the QM cluster is described using the same set of inter-atomic potentials, which was used to generate the amorphous structure in Molecular Dynamics simulations.

We have built several amorphous structures using classical Molecular Dynamics and used the PAS code to analyze their properties and to search for correlations between these properties. The results of this analysis demonstrate that our structures are statistically equivalent to those, obtained in previous calculations. For the first time we applied the embedded cluster method to study defects centers in amorphous SiO_2. The H^+ and H^- centers associated with small (3-member) and large (6-member) rings were considered and their properties were calculated. The results of suggest that there are considerable site variations of the H^+ and H^- defect properties. These variations are larger than those induced by the size and shape of QM clusters used in the calculation and therefore can be studied using the embedded cluster method developed in this project.

References

[1] J. Sarnthein, A. Pasquarello, and R. Car, Phys. Rev. Lett. **74**, 4682 (1995).

[2] A. Pasquarello and R. Car, Phys. Rev. Lett. **80**, 5145 (1998).

[3] J. Sarnthein, A. Pasquarello, and R. Car, Science **275**, 1925 (1997).

[4] G. Pacchioni and G. Ieranò, Phys. Rev. B **57**, 818 (1998).

[5] L. W. Hobbs, C. E. Jesurum, V. Pulim, and B. Berger, Phil. Mag. A **78**, 679 (1998).

[6] A. C. Wright, in *Defects in SiO2 and related dielectrics: Science and Technology*, edited by G. Pacchioni, L. Skuja and D. L. Griscom (Kluwer, Dordrecht, 2000), p. 1.

[7] A. L. Shluger and J. D. Gale, Phys. Rev. B **54**, 962 (1996).

[8] A. L. Shluger, P. V. Sushko, and L. N. Kantorovich, Phys. Rev. B **59**, 2417 (1999).

[9] P. V. Sushko, A. L. Shluger, and C. R. A. Catlow, Surface Sci. **450**, 153 (2000).

[10] P. V. Sushko, A. L. Shluger, R. C. Baetzold, and C. R. A. Catlow, J. Phys.: Condens. Matter **12**, 8257 (2000).

[11] V. B. Sulimov, P. V. Sushko, A. H. Edwards, A. L. Shluger, and A. M. Stoneham, Phys. Rev. B (submitted) (2002).

[12] B. G. Dick and A. W. Overhauser, Phys. Rev. **112**, 90 (1958).

[13] H. Hosono, Y. Ikuta, T. Kinoshita, K. Kajihara, and M. Hirano, Phys. Rev. Lett. **87**, 175501 (2001).

[14] M. A. Szymanski, A. L. Shluger, and A. M. Stoneham, Phys. Rev. B **63**, 224207 (2001).

[15] K. Binder, Comp. Phys. Comm. **121-122**, 168 (1999).

[16] P. Vashishta, R. K. Kalia, J. P. Rino, and I. Ebbsjo, Phys. Rev. B **41**, 12197 (1990).

[17] L. Vollmayr, W. Kob, and K. Binder, Phys. Rev. B **54**, 15808 (1996).

[18] DL_POLY is a package of molecular simulation routines written by W. Smith and T.R. Forester, Copyright the EPSRC acting through its Daresbury and Rutherford Appleton Laboratory at Daresbury Laboratory, 1994.

[19] B. W. H. van Beest, G. J. Kramer, and R. A. V. Santen, Phys. Rev. Lett. **64**, 1955 (1991).

[20] T. Koslowski, W. Kob, and K. Vollmayr, Phys. Rev. B **56**, 9469 (1997).

Contract F61775-00-WE059
Title: First principle calculations of electrical levels for radiation induced defects in amorphous SiO2

This material is based upon work supported by the European Office of Aerospace Research and Development, Air Force Office of Scientific Research, Air Force Research Laboratory, under Contract No. F61775-00-WE059.

Any opinions, findings and conclusions or recommendations expressed in this material are those of the author(s) and do not necessarily reflect the views of the European Office of Aerospace Research and Development, Air Force Office of Scientific Research, Air Force Research Laboratory.

The Contractor, University College London, hereby declares that, to the best of its knowledge and belief, the technical data delivered herewith under Contract No. F61775-00-WE059 is complete, accurate, and complies with all requirements of the contract.

DATE: 21/08/2002

Name and Title of Authorized Official:

Dr. A. Shluger Prof.

I certify that there were no subject inventions to declare as defined in FAR 52.227-13, during the performance of this contract.

DATE: 21/08/2002

Name and Title of Authorized Official:

Dr. A. Shluger Prof.